

KEK Proceedings 2020-2
July 2020
R

Proceedings of the Twenty-Sixth EGS Users' Meeting in Japan

August 4 - 6, 2019.
KEK, Tsukuba, Japan

Edited by

Y. Namito, H. Iwase, Y. Sakaki and H. Hirayama



High Energy Accelerator Research Organization

High Energy Accelerator Research Organization (KEK), 2020

KEK Reports are available from:

High Energy Accelerator Research Organization (KEK)
1-1 Oho, Tsukuba-shi
Ibaraki-ken, 305-0801
JAPAN

Phone: +81-29-864-5137
Fax: +81-29-864-4604
E-mail: irdpub@mail.kek.jp
Internet: <https://www.kek.jp/en/>

FOREWARD

The Twenty-sixth EGS Users' Meeting in Japan was held at High Energy Accelerator Research Organization (KEK) from August 4 to 6. The meeting has been hosted by the Radiation Science Center. More than 30 participants attended the meeting.

The meeting was divided into two parts. Short course on EGS was held at the first half of the workshop using EGS5 code. In the later half, 6 talks related EGS were presented. The talk covered the wide fields, like the medical application and the calculation of various detector responses *etc.* These talks were very useful to exchange the information between the researchers in the different fields.

Finally, we would like to express our great appreciation to all authors who have prepared manuscript quickly for the publication of this proceedings.

Yoshihito Namito
Hiroshi Iwase
Yasuhito Sakaki
Hideo Hirayama
Radiation Science Center
KEK, High Energy Accelerator Research Organization

CONTENTS

- Construction of a Web Application for Calculating Integral Exposure Doses from Cs-137, Cs-134 or K-40 in Wild Animals** 1
D. Endoh, H. Hirayama, H. Ishiniwa, and M. Onuma
- Investigating the Radiation Source Information of CyberKnife SRS/SRT System** 8
K. Masaki, Y. Abe, T. Sagara, H. Endo, Y. Ota, S. Komatsu, S. Komori, R. Kato, H. Ouchi, and T. Kato
- Examination of Evaluation Method of Absorbed Dose of Lenz in Head X-Ray CT** 16
K. Yamazaki, S. Koyama, H. Kimura, and T. Haba
- Use of density effect parameters in ICRU Report 90** 21
Y. Namito, H. Hirayama, and M. Shimizu

CONSTRUCTION OF A WEB APPLICATION FOR CALCULATING INTERNAL EXPOSURE DOSES FROM Cs-137, Cs-134 OR K-40 IN WILD ANIMALS

D Endoh*¹, H Hirayama², H Ishiniwa³ and M Onuma⁴

¹ *Department of Radiation Biology, School of Veterinary Medicine, Rakuno Gakuen University, Ebetsu 069-8501, Japan*

² *Radiation Science Center, KEK, High Energy Accelerator Research Organization, Tsukuba 305-0801, Japan*

³ *Institute of Environmental Radioactivity at Fukushima University, Fukushima 960-1296, Japan*

⁴ *Ecological Risk Assessment and Control Section, Center for Environmental Biology and Ecosystem, National Institute for Environmental Studies, Tsukuba 305-8506, Japan*

E-mail of corresponding author: dendoh@rakuno.ac.jp

Abstract

A user code was made to compute energy depositions on the use of EGS5, and the result of execution in Fortran is output to the result file named egs5job.out. In this execution method, program input and output are performed in a process of writing a file, executing the Fortran-program on a command line, and evaluation of the results with reading the output file. This complicated process has low affinity with the Web-server application. On the other hand, preparing a Fortran execution environment is difficult for biological researchers who want to predict the internal exposure dose. In this research, by using Ruby on Rails (Rails), we constructed an application in which the user code is changed based on the input data of the dynamic Web page, Fortran on the command line is executed by Rails and the output results were analyzed to display the predicted dose rate on a Web page. As a result, it became possible to calculate the beta and gamma-internal exposure doses of Cs-137, Cs-134 and K-40 on the Web application. It is expected that the user code that can predict the beta and gamma-ray internal dose will increase its utility value in the future by linking with script language.

1. Introduction

The National Institute for Environmental Studies has estimated the effects of diffuse radioisotopes on wildlife in the Fukushima Daiichi Nuclear Power Station difficult-to-return area, using the Japanese field mice (*Apodemus speciosus*) as the target animal [1]. At the 2018 EGS Study Group, this research group reported changes in internal exposure dose due to Cs-137 from 2012 to 2016. It is expected that such predictions of internal exposure doses for wild animals will continue to be made while adding target species.

EGS5 has a proven as a method of calculating internal exposure dose with high reliability. On the other hand, one must prepare a computer that runs Fortran-language with basic operating skills for executing EGS5. It is also required to set the radioisotope nuclide, radiation type, elemental composition of body tissue and the size of target tissue in files named as User Code and User Data. The results are displayed in a file constructed by EGS5. In order to obtain the dose rate from the basic output of EGS5 such as energy transfer, recalculation of total energy-transfer in a unit weight of the target-tissues of individuals are needed. Although such an execution and recalculation are sufficiently significant for researchers specializing in simulation research, it is very difficult for usual biologist to handle EGS5-codes and recalculate results. While, high reliability of EGS5 resulted demands of the program for calculating radiation internal doses. There is also a growing need for a method of utilization in which the calculation results are provided to general researchers who are not familiar with simulation software.

In the research on the effects of the accident in Fukushima nuclear plants on wildlife animals, there is a need to predict the internal radiation dose from the specific activity of radionuclides

in/of? animals. While, execution procedures are too difficult for usual biologists. Even a researcher with basic Linux skills may require several years or more to be able to do so. In order to connect the achievements and reliability of EGS5, it is necessary to develop a program interface that is easy for usual biologists to use. If the developer provides a web interface on the server, the user can calculate the internal exposure dose using a web browser regardless of the OS.

In order to run EGS5 on a web server, firstly set the output to text with conditions, then change the user code based on the input on the web server, and then execute the EGS5 program. It is necessary to build a server that executes and reads the output text and displays it on a web page. By using current technologies such as HTML, XML, jQuery, etc., these operations are basically possible, but since the procedure for development is complicated, in order to develop with limited personnel and funds, it is necessary to utilize the development support package for Web pages. In this research, using the Web page development support package Ruby on Rails, the internal exposure dose due to beta rays and gamma rays is calculated from the specific activity of Cs-137, Cs-134 and K-40 of the mouse, which is supposed to be a cylinder. In this study, some points on the application development were described.

2. Materials and Methods

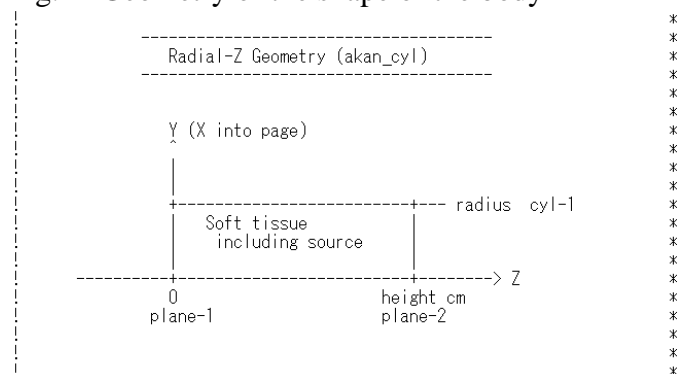
2.1 Radiation measurements of Mice

Mice were captured by traps in the Fukushima Daiichi NPP difficult-to-return area, and Cs-137 gamma rays were measured by a germanium measuring instrument for part of the body tissue after euthanasia. For Cs-137 beta ray and gamma ray, it was calculated by EGS 5 based on the amount of Cs-137 in body tissue calculated based on the frequency of measured gamma rays. With respect to Cs-134 and K-40, radiation dose was not calculated, since there was no measurement result.

2.2 User code

For the beta and gamma-ray energy distribution of Cs-137, Cs-134 and K-40, we referred to ICRP Publication 107. As the geometry for calculating the internal exposure, a cylindrical body was assumed as the body of the mouse, and the radiation source was dispersed throughout the body, and the shape of the whole body was the measuring instrument (Fig. 1).

Fig. 1 Geometry of the shape of the body



On the settings of the User Code for calculating the internal exposure dose, the energy distribution of each nuclide is described in the section for the beta and gamma-ray energy settings (Fig. 2). Depending on the choice of beta or gamma-rays set, they were loaded into a set array for calculation of beta or gamma-rays (Fig. 3). Next, the EGS5-call section was used to read information about murine substances, and the Shower-call section that specified beta rays or gamma-rays were generated in random directions at random positions in the cylinder (Fig. 4). Regarding the energy absorbed in the substance, the code for totaling in the entire cylinder is described in the Output-of-results section (Fig. 5).

Fig. 2 Beta and gamma-ray energy settings in user code

A. Settings for basic variables

real*8↓

```
* ebeta(74),pbeta(74),cbeta(74),egamma(16),pgamma(16),cgamma(16),↓  
* ebc137(60),pbc137(60),egc137(3),pgc137(3),ebc134(74),↓  
* pbc134(74),egc134(9),pgc134(9),ebk40(67),pbk40(67),↓  
* egk40(16),pgk40(16) ↓
```

B. Beta-ray energy-settings

Cs-137

```
ICRP 107 Cs-137 beta data  
data ebc137/0.00000,0.02000,0.04000,0.06000,0.08000,0.10000,  
* 0.12000,0.14000,0.16000,0.18000,0.20000,0.22000,0.24000,  
* 0.26000,0.28000,0.30000,0.32000,0.34000,0.36000,0.38000,  
* 0.40000,0.42000,0.44000,0.46000,0.48000,0.50000,0.52000,  
* 0.54000,0.56000,0.58000,0.60000,0.62000,0.64000,0.66000,  
* 0.68000,0.70000,0.72000,0.74000,0.76000,0.78000,0.80000,  
* 0.82000,0.84000,0.86000,0.88000,0.90000,0.92000,0.94000,  
* 0.96000,0.98000,1.00000,1.02000,1.04000,1.06000,1.08000,  
* 1.10000,1.12000,1.14000,1.16000,1.17563/  
  
data pbc137/0.0,0.67579E-01,0.64985E-01,0.63006E-01,0.61128E-01,  
* 0.59349E-01,0.57611E-01,0.55874E-01,0.54112E-01,0.52270E-01,  
* 0.50313E-01,0.48206E-01,0.45909E-01,0.43403E-01,0.40647E-01,  
* 0.37622E-01,0.34327E-01,0.30723E-01,0.26949E-01,0.23041E-01,  
* 0.18999E-01,0.15080E-01,0.11283E-01,0.76665E-02,0.51303E-02,  
* 0.27741E-02,0.15107E-02,0.13401E-02,0.11878E-02,0.11448E-02,  
* 0.11199E-02,0.10934E-02,0.10651E-02,0.10363E-02,0.10046E-02,  
* 0.97242E-03,0.93808E-03,0.90157E-03,0.86451E-03,0.82409E-03,  
* 0.78312E-03,0.74002E-03,0.69481E-03,0.64918E-03,0.60104E-03,  
* 0.55247E-03,0.50299E-03,0.45258E-03,0.40218E-03,0.35178E-03,  
* 0.30138E-03,0.25514E-03,0.21306E-03,0.17098E-03,0.12890E-03,  
* 0.86818E-04,0.57081E-04,0.39686E-04,0.22292E-04,0.53119E-05/
```

Cs-134

```
ICRP 107 Cs-134 beta data  
data ebc134/0.0000000,0.0200000,0.0400000,0.0600000,  
* 0.0800000,0.1000000,0.1200000,0.1400000,0.1600000,0.1800000,  
* 0.2000000,0.2200000,0.2400000,0.2600000,0.2800000,0.3000000,  
* 0.3200000,0.3400000,0.3600000,0.3800000,0.4000000,0.4200000,  
* 0.4400000,0.4600000,0.4800000,0.5000000,0.5200000,0.5400000,  
* 0.5600000,0.5800000,0.6000000,0.6200000,0.6400000,0.6600000,  
* 0.6800000,0.7000000,0.7200000,0.7400000,0.7600000,0.7800000,  
* 0.8000000,0.8200000,0.8400000,0.8600000,0.8800000,0.9000000,  
* 0.9200000,0.9400000,0.9600000,0.9800000,1.000000,1.020000,  
* 1.040000,1.060000,1.080000,1.100000,1.120000,1.140000,1.160000,  
* 1.180000,1.200000,1.220000,1.240000,1.260000,1.280000,1.300000,  
* 1.320000,1.340000,1.360000,1.380000,1.400000,1.420000,1.440000,  
* 1.453780/  
data pbc134/0.0,0.18060,0.12348,0.79063E-01,0.50203E-01,  
* 0.39790E-01,0.38836E-01,0.38081E-01,0.37182E-01,0.36118E-01,  
* 0.34919E-01,0.33590E-01,0.32132E-01,0.30563E-01,0.28884E-01,  
* 0.27116E-01,0.25288E-01,0.23394E-01,0.21466E-01,0.19528E-01,  
* 0.17579E-01,0.15665E-01,0.13785E-01,0.11922E-01,0.10161E-01,  
* 0.84174E-02,0.68072E-02,0.53309E-02,0.39071E-02,0.27984E-02,  
* 0.17422E-02,0.97771E-03,0.50488E-03,0.89852E-04,0.21621E-04,  
* 0.11190E-04,0.56274E-05,0.49328E-05,0.42461E-05,0.36068E-05,  
* 0.29754E-05,0.24275E-05,0.19631E-05,0.15361E-05,0.13336E-05,  
* 0.11686E-05,0.10672E-05,0.10296E-05,0.99202E-06,0.95442E-06,  
* 0.91681E-06,0.87571E-06,0.83111E-06,0.78651E-06,0.74190E-06,  
* 0.69730E-06,0.65053E-06,0.60157E-06,0.55261E-06,0.50365E-06,  
* 0.45470E-06,0.40675E-06,0.35982E-06,0.31288E-06,0.26595E-06,  
* 0.21901E-06,0.17894E-06,0.14574E-06,0.11253E-06,0.79324E-07,  
* 0.46117E-07,0.24026E-07,0.13050E-07,0.26052E-08/
```

K-40

```
ICRP 107 K-40 beta data  
data ebk40/0.000000,0.200000E-01,0.400000E-01,0.600000E-01,  
* 0.800000E-01,0.100000,0.120000,0.140000,0.160000,  
* 0.180000,0.200000,0.220000,0.240000,0.260000,0.280000,  
* 0.300000,0.320000,0.340000,0.360000,0.380000,0.400000,  
* 0.420000,0.440000,0.460000,0.480000,0.500000,0.520000,  
* 0.540000,0.560000,0.580000,0.600000,0.620000,0.640000,  
* 0.660000,0.680000,0.700000,0.720000,0.740000,0.760000,  
* 0.780000,0.800000,0.820000,0.840000,0.860000,0.880000,  
* 0.900000,0.920000,0.940000,0.960000,0.980000,1.000000,  
* 1.020000,1.040000,1.060000,1.080000,1.100000,1.120000,  
* 1.140000,1.160000,1.180000,1.200000,1.220000,1.240000,  
* 1.260000,1.280000,1.300000,1.311090/  
data pbk40/0.0,0.82355E-02,0.88810E-02,0.96295E-02,0.10351E-01,  
* 0.11035E-01,0.11683E-01,0.12301E-01,0.12888E-01,0.13446E-01,  
* 0.13980E-01,0.14487E-01,0.14968E-01,0.15423E-01,0.15852E-01,  
* 0.16255E-01,0.16631E-01,0.16973E-01,0.17295E-01,0.17589E-01,  
* 0.17855E-01,0.18090E-01,0.18295E-01,0.18492E-01,0.18643E-01,  
* 0.18786E-01,0.18898E-01,0.18977E-01,0.19047E-01,0.19066E-01,  
* 0.19077E-01,0.19052E-01,0.18993E-01,0.18925E-01,0.18804E-01,  
* 0.18673E-01,0.18507E-01,0.18306E-01,0.18095E-01,0.17828E-01,  
* 0.17552E-01,0.17237E-01,0.16885E-01,0.16521E-01,0.16095E-01,  
* 0.15658E-01,0.15149E-01,0.14568E-01,0.13987E-01,0.13405E-01,  
* 0.12824E-01,0.12131E-01,0.11327E-01,0.10522E-01,0.97177E-02,  
* 0.89132E-02,0.80211E-02,0.70414E-02,0.60617E-02,0.50819E-02,  
* 0.41022E-02,0.32568E-02,0.25457E-02,0.18346E-02,0.11235E-02,  
* 0.41240E-03,0.15761E-04/  
* 0.46117E-07,0.24026E-07,0.13050E-07,0.26052E-08/
```

C. gamma-energy settings

```
ICRP 107 Cs-137 gamma data
data egcs137/0.0332,0.0364,0.662/
data pgcs137/0.056,0.013,0.851/

ICRP 107 Cs-134 gamma data
data egcs134/4.754E-01,5.632E-01,5.693E-01,6.047E-01,
* 7.959E-01,8.020E-01,1.039E+00,1.168E+00,1.365E+00/
data pgcs134/1.49E-02,8.35E-02,1.54E-01,9.76E-01,
* 8.55E-01,8.69E-02,9.88E-03,1.79E-02,3.01E-02/

ICRP 107 K-40 gamma data
data egk40/2.928E-03,2.931E-03,3.163E-03,3.163E-03,6.400E-05,
* 6.634E-05,2.988E-04,2.990E-04,2.340E-06,2.205E-04,
* 2.350E-04,2.182E-04,2.325E-04,2.327E-04,5.110E-01,
* 1.461E+00/
data pgk40/2.96E-03,5.85E-03,2.42E-04,4.79E-04,5.02E-06,1.35E-05,
* 3.92E-06,6.19E-06,9.61E-14,2.97E-05,1.28E-08,6.10E-05,
* 1.30E-08,1.28E-08,1.80E-03,1.07E-01/
```

Fig. 3 Selection of nucleotide and codes for calculation

```
write(6,'(A)') ' Isotope 0: Cs-137, 1: Cs-134, 2: K-40' ↓
read(5,*) nuclide ↓

if(nuclide.eq.0) then ↓
  if(istype.eq.0) then ↓
    nbeta=60 ↓
    do i=1,nbeta ↓
      ebeta(i)=ebcs137(i) ↓
      pbeta(i)=pbcs137(i) ↓
    end do ↓
  else ↓
    ngamma=3 ↓
    do i=1,ngamma ↓
      egamma(i)=egcs137(i) ↓
      pgamma(i)=pgcs137(i) ↓
    end do ↓
  end if ↓
elseif(nuclide.eq.1) then ↓
  if(istype.eq.0) then ↓
    nbeta=74 ↓
    do i=1,nbeta ↓
      ebeta(i)=ebcs134(i) ↓
      pbeta(i)=pbcs134(i) ↓
    end do ↓
  else ↓
    ngamma=9 ↓
    do i=1,ngamma ↓
      egamma(i)=egcs134(i) ↓
      pgamma(i)=pgcs134(i) ↓
    end do ↓
  end if ↓
else ↓
  if(istype.eq.0) then ↓
    nbeta=67 ↓
    do i=1,nbeta ↓
      ebeta(i)=ebk40(i) ↓
      pbeta(i)=pbk40(i) ↓
    end do ↓
  end if ↓
end if ↓
```


Fig. 4 Setting the radiation source positions

```

-----
! Step 6: Initialization-for-howfar
-----
! Define various thicknesses/distances
  if(igeo.eq.0) then ! cylinder
! Definition of planes

! Set zbound to zero to begin with
  zbound(1)=0.0

! Now put in the exceptions

  zbound(2)=otissue
  zbound(3)=zbound(2)+height
  zbound(4)=zbound(3)+otissue

  write(6,'(A)') ' Zbound for each j-plane (i=1,3):'
  do j=1,nplan
    write(6,'(I5,G15.7)') j,zbound(j)
  end do

! Define the cylinder radii

  cyrad(1)=radius
  cyrad(2)=cyrad(1)+otissue

! Print out the cylinder radii
  write(6,'(A)') ' cylinder radii'
  do i=1,ncyl
    cyrad2(i)=cyrad(i)*cyrad(i)
    write(6,'(A,I5,A,G15.5,A)')
  * ' i=',i,' cyrad(i)=' ,cyrad(i),' cm'
  end do
  else ! sphere
! Define sphere radius
  sprad(1)=radius
  sprad(2)=sprad(1)+otissue
! Print out the cylinder radii
  write(6,'(A)') ' Sphere radii'
  do i=1,nsph
    sprad2(i)=sprad(i)*sprad(i)
    write(6,'(A,I5,A,G15.5,A)')
  * ' i=',i,' sprad(i)=' ,sprad(i),' cm'
  end do
  end if
end if

```

Fig.5

```

-----
! Step 9: Output-of-results
-----
  write(6,'(A,I10,A/A,I10,A/A,G15.5,A)')
  * ' Ncount=', ncount,' (actual cases run)',
  * ' Ncases=',ncases,' (number of cases requested)',
  * ' TotKE =',totke,' (total KE (MeV) in run)'

  if (totke .le. 0.00) then
    write(6,'(A,G15.5/A,G15.5,A,I10)')
  * ' Stopped in MAIN with TotKE=',totke,
  * ' AvailKE=',availke,' Ncount=',ncount
  stop
  end if

  if(istype.eq.0) then
  if(nuclide.eq.0) then
    write(6,'(A)') ' Results for Cs-137 beta-ray'
    write(2,'(A)') ' Cs-137 beta-ray'
  elseif(nuclide.eq.1) then
    write(6,'(A)') ' Results for Cs-134 beta-ray'
    write(2,'(A)') ' Cs-134 beta-ray'
  else
    write(6,'(A)') ' Results for K-40 beta-ray'
    write(2,'(A)') ' K-40 beta-ray'
  end if
  else
  if(nuclide.eq.0) then
    write(6,'(A)') ' Results for Cs-137 gamma-ray'
    write(2,'(A)') ' Cs-137 gamma-ray'
  elseif(nuclide.eq.1) then
    write(6,'(A)') ' Results for Cs-134 gamma-ray'
    write(2,'(A)') ' Cs-134 gamma-ray'
  else
    write(6,'(A)') ' Results for K-40 gamma-ray'
    write(2,'(A)') ' K-40 gamma-ray'
  end if
  end if

  if(igeo.eq.0) then ! cylinder
    write(6,'(A,F10.3,A,F10.3,A)') ' Organ radius =',
  * radius,' cm radius and ',height,' cm height cylinder'
    write(2,'(A,F10.3,A,F10.3,A)') ' Organ radius =',
  * radius,' cm radius and ',height,' cm height cylinder'
  else ! sphere
    write(6,'(A,F10.3,A,F10.3,A)') ' Organ sphre radius =',
  * radius,' cm'
    write(2,'(A,F10.3,A,F10.3,A)') ' Organ sphre radius =',
  * radius,' cm'
  end if
end if

```

2.3 Output settings for calculation results

As an execution setting of EGS5, a file called `akan_3.f` was set to read various sizes of radiation, radioisotope and body tissue called `akan_3_s.data` (Fig. 6). With this setting, once `akan_3.f` was executed on the command line, then by changing `akan_3_s.data`, the dose under various conditions was calculated. The output was set so that only the data needed by the biologist to calculate the internal exposure was output to the file `egs5job.ou2`.

Fig. 6 Output file settings in

```
1, 0, 1, 5.0, 10.0, 10.0

1      ! 0:beta, 1:gamma
```

2.4 Web interface

Ruby on Rails (Rails) 2.5 was used as the software for the Web interface. The main body of EGS5 and the setting file were placed in the 'lib' folder of Rails. Radius and height of the cylinder was set in `akan_3_s.data` file according to the Web-page created by Rails. The conditions are displayed as a list, and the calculation under the condition selected by the researcher is executed by clicking a link next to the displayed conditions. Calculation procedures proceeded according to the ruby codes in Controller section of Rails (Fig. 7).

Fig. 7 Controller section of Rails

```
<h1>Conditions</h1>
Input variables: Input numbers in each textbox<br>
Radiation. 0:beta, 1:gamma<br>
RI.      0: Cs-137, 1: Cs-134, 2: K-40<br>
Shape (Shape of target organ). 0: Cylinder  other: Sphere<br>
Radius.  Radius of target organ in cm<br>
Height.  Height of target organ assuming cylinder in cm<br>
Tissue.  Tissue size outside cylinder in cm<br>
<br>
<table>
  <thead>
    <tr>
      <th>Radiation</th>
      <th>RI</th>
      <th>Shape</th>
      <th>Radius</th>
      <th>Height</th>
      <th>Tissue</th>
      <th colspan="3"></th>
    </tr>
  </thead>
  <tbody>
    <% @conditions.each do |condition| %>
      <tr>
        <td><%= condition.radiation %></td>
        <td><%= condition.ri %></td>
        <td><%= condition.shape %></td>
        <td><%= condition.radius %></td>
        <td><%= condition.height %></td>
        <td><%= condition.tissue %></td>
        <td><%= link_to 'Calculate Dose', condition %></td>
        <td><%= link_to 'Edit', edit_condition_path(condition) %></td>
        <td><%= link_to 'Destroy', condition, method: :delete, data: { confirm: 'Are you sure?' } %></td>
      </tr>
    <% end %>
  </tbody>
</table>
<br>
```

3. Results and Discussions

The constructed program was confirmed to run on the local machine. On the local machine or server, it is necessary to run EGS5 from the command line once, while after that, it only worked with the web interface. Due to this execution specification, it was suggested that after the program was set up, it could be used by standard biologists.

In the EGS5 User Code, a basic internal exposure measurer was created by describing the energy distribution and the code that randomly sets the source distribution and direction (Fig. 6). This internal exposure measurement system can be changed for different types of radiation (beta or gamma rays), and calculation for each nuclide is also possible by setting an argument as a command. By expanding this user code, the command input from EGS5 can be set by the Web program, and

the internal exposure effects of various nuclides can be calculated without executing Fortran on the terminal.

At present, the biological effect of Cs-137 is the focus, but the effect of Cs-134 remains on some sampling schedules. Maintenance is required. K-40 can be used as a background for the effects of radioisotopes in the body. This program has achieved the intended purpose. However, due to the ease of operation, it is necessary to consider cases where it is used for purposes other than expected, and functions to control access of users may be required.

4. References

[1] D Endoh, D., Hirayama, H., Ishiniwa H. and Onuma, M. "Prediction of internal exposure by Cs-137 of randomly collected in difficult-to-recover area of Fukushima dai-ichi NPS 2 - EGS5 user code and internal exposure calculation from 2012 to 2016-" (KEK, Tsukuba, Japan). 2018.

Investigating the radiation source information of CyberKnife SRS/SRT system.

K. Masaki¹, Y. Abe¹, T. Sagara¹, H. Endo¹, Y. Ota¹,
S. Komatsu¹, S. Komori¹, R. Kato¹, H. Ouchi¹ and T. Kato¹⁻²

*¹Department of Radiation Physics and Technology,
Southern Tohoku Proton Therapy Center, Koriyama 963-8052, Japan.*

*²Preparing Section for New Faculty of Medical Science,
Fukushima Medical University, Fukushima 960-1295, Japan.*

e-mail: wurstp38@yahoo.co.jp

Abstract

CyberKnife (Accuray Inc., Sunnyvale, CA) is a radiation therapy device focused on high-precision radiation therapy. In the treatment using CyberKnife, the dose gradient is steep across the shape of the target or healthy tissues. Because of this, the accuracy of dose calculation is particularly important. To perform accurate dose calculations, it is necessary to obtain reliable radiation source information; therefore, the aim of this study was to obtain reliable radiation source information of CyberKnife, for use it in Monte Carlo (MC) dose calculations. The source information was obtained through the MC simulation in the treatment machine head of CyberKnife. The geometrical details were obtained from manufacturers' specifications. Accelerated electrons were impinged on the X-ray target, and the information of particles output from the device was recorded in the form of IAEA phase space data (PSD). The validity of obtained PSDs was verified through the comparison of calculated water dose distribution and measurements. The radiation beam was incident perpendicular to the surface of water with source-to-surface distance of 80 cm. The percentage depth dose (PDD) and off-center ratio (OCR) were calculated and measured. The comparison of PDDs, calculated values agreed with measurements within 1 mm distance-to-agreement (DTA) value in the build-up region and agreed within almost 1% local error in the depth beyond the build-up region. Also, the calculated OCRs agreed with measurements within almost 2% local errors in the radiation fields and agreed within 1 mm DTA value in the penumbra region. These

results showed that the obtained PSDs have the validity for use it in dose calculations.

1. Introduction

CyberKnife (Accuray Inc., Sunnyvale, CA), one of the radiation therapy devices, is specialized in stereotactic radiosurgery (SRS) and stereotactic radiation therapy (SRT). In SRS or SRT, a high dose is delivered to targets in one or few treatment fractions in order to achieve good clinical outcomes in a short period. To irradiate a target with a high dose while reducing the toxicity to healthy tissues, high accuracy is required for treatment planning and radiation delivery. The CyberKnife system consists of a linear accelerator mounted to a robotic manipulator and a digital X-ray imaging device, and it can perform multi-directional irradiation with high accuracy for a small target such as a brain tumor.

In radiation therapy, dose distributions in the patients are calculated to develop optimal treatment plans for each clinical case. In SRS and SRT, the dose calculation accuracy is particularly important because treatment is performed with a steep dose distribution which conforms to the shape of the target or healthy tissues. It is widely known that Monte Carlo (MC) method is the most accurate dose calculation algorithm¹; however, full-MC method, which does not include variance reduction techniques² or parameter discretization, is not used clinically in most cases due to the long computational time. Instead of full-MC method, correction-based algorithms that calculate dose distributions by applying correction factors to the standard measurement data in water and physical model-based analytical dose calculation algorithms such as a convolution method are the mainstream in clinical situations¹. However, these algorithms cause calculation errors due to the theoretical limits of inhomogeneity correction. Therefore, it is useful that there is an independent verification tool which recalculates treatment plans using full-MC method.

To perform accurate dose calculations, it is necessary to obtain reliable radiation source information (e.g., energy spectrum and fluence map). In photon therapy using a clinical linear accelerator, output photons and electrons have a wide range of energies up to several MeV. In addition, the dose rates of treatment beams are very high. For these reasons, it is difficult to obtain reliable radiation source information by direct measurement³⁻⁴. Alternatively, several studies have reported the methods for obtaining it through MC simulations⁵⁻⁹. The aim of this study was to obtain reliable radiation source information of CyberKnife SRS/SRT system through MC simulations, for use it in MC dose calculations.

2. Materials and methods

2.1 The MC simulation of CyberKnife treatment machine head.

We simulated CyberKnife M6 series (Accuray) with the fixed circular collimators. Simulations were performed by using EGS5¹⁰. The geometrical details of the machine head were obtained from manufacturers' specifications. The schematic overview of simulations is shown in Fig. 1.

Firstly, the simulation 1 which is from the X-ray target plane to scoring plane 1 was performed. This simulation is a common part independent of the type of fixed circular collimators. The energy of incident electrons is monoenergetic 7.3 MeV. Also, the fluence map of electrons on the X-ray target plane was determined by the Gaussian distribution with $\sigma = 1.15$ mm. The information of particles reached the scoring plane 1 was recorded in the form of International Atomic Energy Agency (IAEA) phase-space data (PSD)¹¹. The recorded information was particle charge (iq), energy (e), position (x,y) and direction vector (u,v). The position (z) and direction vector (w) were not recorded because these variables are known or can be calculated using other variables. The cut-off energies AE and AP in this simulation were 0.700 MeV and 0.010 MeV, respectively.

Secondly, the simulation 2 which is from the upstream of fixed circular collimators to scoring plane 2 was performed. There are 12 types of fixed circular collimators with diameters ranging from 5 mm to 60 mm at the source-to-axis distance of 80 cm plane. Since the simulation geometry differs for each collimator, the PSD recorded at the scoring plane 1 was used as a radiation source of these simulations, and the particles passed through each collimator were recorded at the scoring plane 2. Recorded particle information and cut-off energies were the same as in the simulation 1.

2.2 Comparison of calculated and measured water dose distributions.

The validity of obtained PSDs was verified through the comparison of calculated water dose distribution and measurements. The MP3 water scanning system (PTW, Freiburg, Germany) and type-60012 diode detector (PTW) were used for the measurements. The radiation beam was incident perpendicular to the phantom surface with source-to-surface distance of 80 cm. The percentage depth dose (PDD) and off-center ratio (OCR) in the depth of 1.5 cm, 5.0 cm, 10.0 cm, 20.0 cm and 30.0 cm were measured.

In the MC dose calculation, a virtual water phantom, whose mass density is homogeneous 1.0 g/cm^3 , was created using a voxel user code in EGS5¹². The phantom size was set to $40 \times 40 \times 40 \text{ cm}^3$, which was large enough not to disturb the charged-particle equilibrium. The PSDs obtained for each field at the scoring plane 2

were used for dose calculations as a radiation source. The calculation grid size was set to $2 \times 2 \times 2 \text{ mm}^3$ for PDD calculations and $1 \times 1 \times 1 \text{ mm}^3$ for OCR calculations. The statistical uncertainty was less than 0.5% at the depth of 10.0 cm on the beam axis. The cut-off energies AE and AP were 0.521 MeV and 0.010 MeV, respectively.

3 Results

The results of comparing calculated water dose distributions and measurements for 10 mm and 60 mm diameters from 12 different sized collimators are obtained. The diameter of 60 mm is the reference field size for CyberKnife, and the diameter of 10 mm is a field size often used for the treatment such as a brain tumor.

The comparison between calculated and measured PDDs is shown in Fig. 2. In both field sizes, calculated values agreed with measurements within 1 mm distance-to-agreement (DTA) value, which is the nearest distance from a point of a reference dose to the point of the same amount of dose, in the build-up region. Also, calculated values agreed within almost 1% local error in the depth beyond the build-up region. According to the IAEA technical report¹³⁾, the recommend tolerances are within 10% local errors or 2 mm DTA values in the build-up region, and within 2% local errors in the depth beyond the build-up region. Calculation errors were within these tolerances.

The comparison between calculated and measured OCRs is shown in Fig. 3. In both radiation fields, calculated values agreed with measurements within almost 2% local errors in the radiation fields. In the penumbra region, calculated values agreed within 1 mm DTA value. The recommended tolerances are within 3% local errors in the radiation field, and within 10% local errors or 2 mm DTA values in the penumbra region. As with the PDD comparison, the calculation errors were within these tolerances.

4 Discussion

The parameter of incident electrons in the treatment machine head simulation was determined with reference to previous studies⁸⁻⁹⁾. Firstly, we performed the simulation with the electron parameter provided by Ma et al.⁸⁾, whose parameter was that energy is monoenergetic 6.8 MeV and the fluence map is the Gaussian distribution with $\sigma = 1.15 \text{ mm}$. As a result, the calculated PDD caused an error suggesting that the beam energy was too low. The details of the device model were not described; however, it

seems to be an older model than CyberKnife M6 series because of published year of the paper. In addition, since there are individual differences between devices, it is considered that there might be some differences in the parameters of incident electrons. Based on the parameter provided by Ma et al., adjustments were made by trial and error to match the characteristics of our device. The relationship between incident electron energy and calculated PDDs with the diameter of 60 mm collimator are shown in Fig. 4. The simulations with several electron energies were performed, and the parameter for which calculation errors become a plateau was determined. It took about one week from the simulation to obtain PSDs to the calculation of water dose distributions with a sufficiently small statistical uncertainty by using Core i7-8700K CPU (Intel Corporation, Santa Clara, CA). Due to the long computational time, it is not practical to use optimization algorithm such as a newton's method; therefore, the parameters were determined by the method described above. Finally, the good agreement was obtained between calculated and measured dose distributions. In regions with a high dose gradient such as build-up and penumbra regions, the calculated profiles appear to be blunter than the measurements. This is due to the difference between the calculation grid size and the sensitive volume of the diode detector, whose sensitive volume size was 0.03 mm^3 . Since the diode detector has a much smaller sensitive volume, it is natural that the sharper profile of the measurements was observed.

5 Conclusion

We performed MC simulations of CyberKnife SRS/SRT system to obtain the radiation source information. Obtained source information was used for calculating water dose distributions and was compared with measurements. Calculated dose distributions were in good agreement with measurements; therefore, it was showed that the obtained source information has the validity for use it in dose calculations.

Acknowledgments

The authors are grateful to Accuray Inc. for providing the specifications of CyberKnife M6 series for MC simulations.

References

- 1) AAPM, “Tissue inhomogeneity corrections for megavoltage photon beams”, AAPM report No. 85 Task Group No. 65 (2004).
- 2) A. Bielajew and D. Rogers, “Lecture notes: Variance Reduction Techniques”, National Research Council of Canada report PIRS-0396 (1994).
- 3) P. H. Huang, K. R. Kase and B. E. Bjärngard, “Spectral characterization of 4 MV Bremsstrahlung by attenuation analysis”, *Med. Phys.* 8, 368–374 (1980).
- 4) P. H. Huang, K. R. Kase and B. E. Bjärngard, “Reconstruction of 4-MV bremsstrahlung spectra from measured transmission data”, *Med. Phys.* 10, 778–785 (1982).
- 5) R. Mohan, C. Chui and L. Lidofsky, “Energy and angular distributions of photons from medical linear accelerators”, *Med. Phys.* 12, 592–597 (1985).
- 6) G. X. Ding, “Energy spectra, angular spread, fluence profiles and dose distributions of 6 and 18 MV photon beams: results of Monte Carlo simulations for a Varian 2100EX accelerator”, *Phys. Med. Biol.* 47, 1025–1046 (2002).
- 7) J. Deng, S. B. Jiang, A. Kapur, J. Li, T. Pawlicki and C. M. Ma, “Photon beam characterization and modelling for Monte Carlo treatment planning”, *Phys. Med. Biol.* 45, 411–427 (2000).
- 8) C. M. Ma, J. S. Li, J. Deng and J. Fan, “Implementation of Monte Carlo Dose Calculation for CyberKnife treatment planning”, *Journal of Physics: Conference Series* 102, 1–10 (2008).
- 9) P. Francescon, S. Cora and C. Cavedon, “Total scatter factors of small beams: a multidetector and Monte Carlo study”, *Med. Phys.* 35, 504–513 (2008).
- 10) H. Hirayama, Y. Namito, A.F. Bielajew, S. J. Wilderman and W. R. Nelson, “The EGS5 Code System”, SLAC-R-730 (2005) and KEK Report 2005-8 (2005).
- 11) IAEA, “Phase-Space Database for External Beam Radiotherapy. Summary Report of a Consultants’ Meeting”, IAEA Report INDC (NDS)-0484 (2006).
- 12) H. Hirayama and Y. Namito, “Lecture Notes of Dose distribution calculation inside phantom with Voxel”, KEK Report 2011-8 (2011).
- 13) IAEA, “Commissioning and Quality Assurance of Computerized Planning Systems for Radiation Treatment of Cancer”, Technical Reports Series No. 430 (2004).

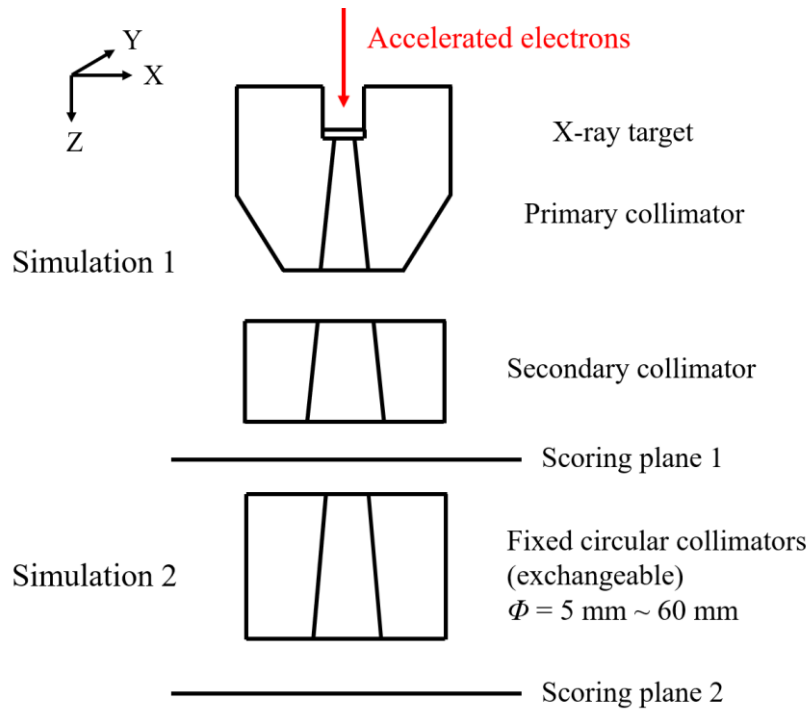


Fig. 1. The schematic overview of machine simulations.

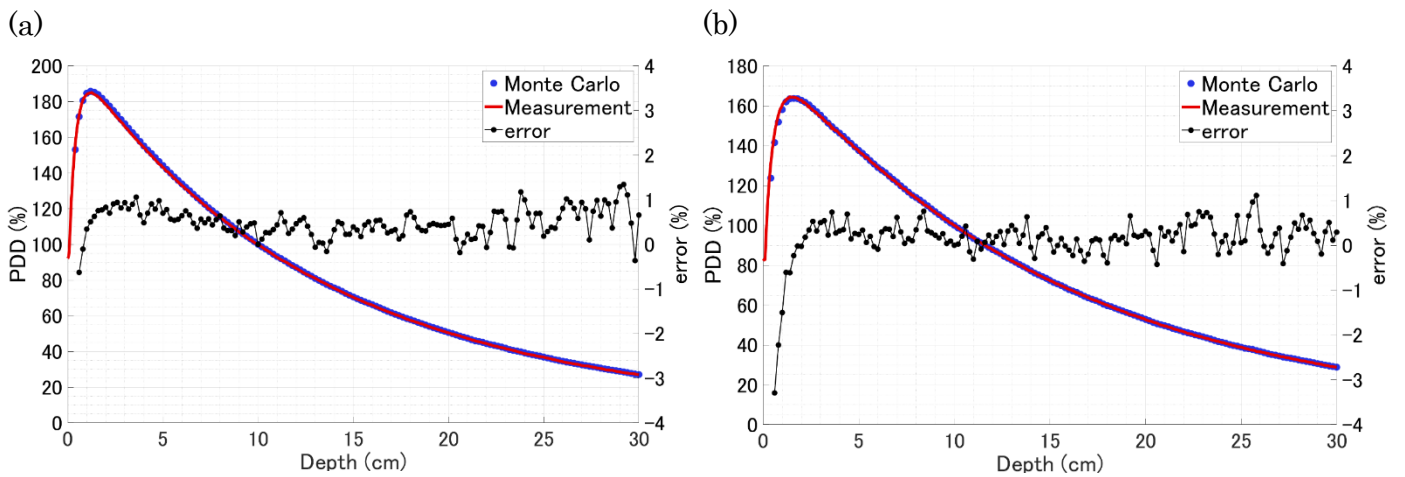


Fig. 2. The comparison of calculated PDDs and measurements.

(a) $\phi = 10 \text{ mm}$. (b) $\phi = 60 \text{ mm}$.

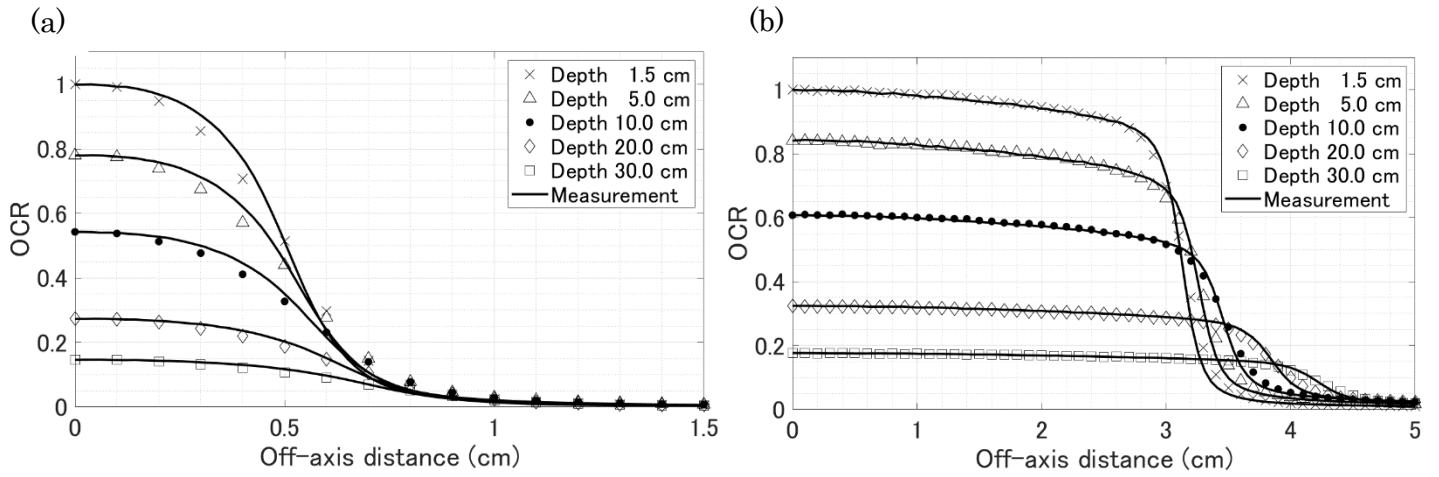


Fig. 3. The comparison of calculated OCRs and measurements.

(a) $\phi = 10$ mm. (b) $\phi = 60$ mm.

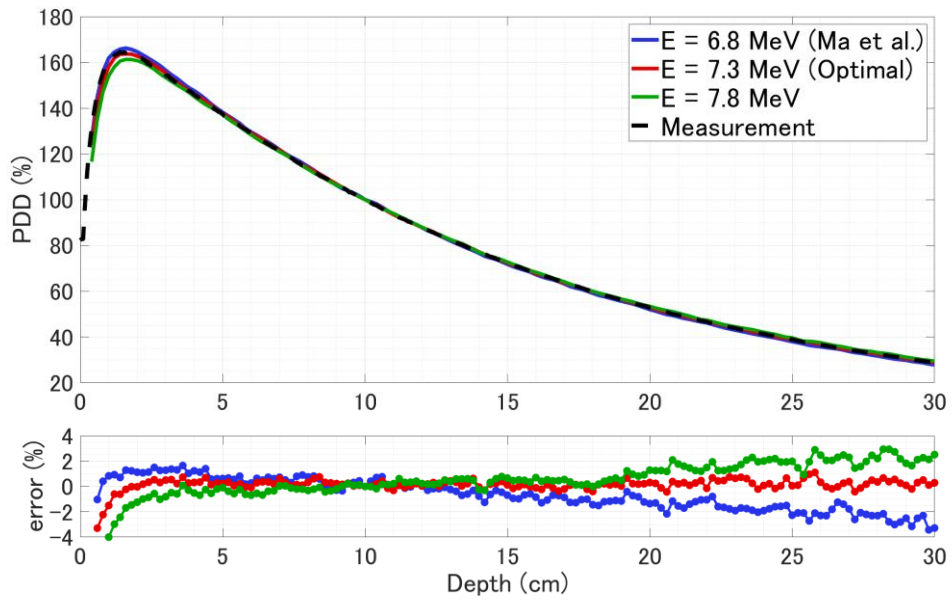


Fig. 4. The relationship between incident electron energy and calculated PDDs.

EXAMINATION OF EVALUATION METHOD OF ABSORBED DOSE OF LENS IN HEAD X-RAY CT

K.Yamazaki¹, S.Koyama², H.Kimura¹, and T.Haba³

¹*Department of Radiological Technology, Graduate School of Medicine, Nagoya University
1-1-20 Daikou-Minami, Higashi-ku, Nagoya 461-8673, Japan*

²*Brain and Mind Research Center*

1-1-20 Daikou-Minami, Higashi-ku, Nagoya 461-8673, Japan

³*Fujita Health University, Faculty of Radiological Technology, School of Medical Science
1-98 Dengakugakubo, Kutsukake-cho, Toyoake, Aichi 470-1192, Japan*

Abstract

Japan is one of the countries with the highest medical exposure in the world. In addition, most medical exposure is accounted for X-ray computed tomography (CT) examinations. In the head CT examination, lens dose is regarded as a problem, and in the lens dose measurement, evaluation is performed by installing a dosimeter on the surface of the phantom. With this method, however, the dose measurement positions of the lens and dosimeter are different, so accurate dose measurement is considered difficult. In this study, the difference of absorbed dose between the lens and the dosimeter puts on the eyelid surface was calculated and compared using Monte Carlo Simulation (EGS5 : Electron Gamma Shower [1]). As a result, the absorbed dose ratio between them was about 0.8. Even in actual measurements, it is considered that the dose of lens is smaller than the dose on the eyelid surface.

1. Introduction

X-ray computed tomography (CT) examination is indispensable in modern medicine. In Japan, a large number of X-ray CT units are used compared to countries around the world. Most of the medical exposure is due to X-ray CT examination. Japan is, therefore, the country with the highest medical exposure in the world. In order to control medical exposure, it is first necessary to know the exposure dose from the examination. In the X-ray examination the exposure dose is measured using dosimeters put in or on the surface of a phantom that simulates the human body. In particular, the dose to the surface organs of the human body is often evaluated by the dose measured with the dosimeter placed on the surface. In general X-ray examinations, the exposure dose decreases with increasing depth from the surface. In the X-ray CT, the dose distribution in the phantom is estimated to be complicated due to the rotary irradiation system. In this study, we focused on the lens dose in the head X-ray CT and examined the difference between the absorbed dose of the lens and the absorbed dose of dosimeter put on the eyelid surface using Monte Carlo simulation (EGS5 : Electron Gamma Shower [1]).

2. Materials and Methods

In this study, we used EGS5 (Electron Gamma Shower 5) and performed a simulation assuming head X-ray CT.

2.1 X-ray CT unit

We modeled an Aquilion ONE made by CANON MEDIACL SYSTEMS as X-ray CT unit and simulated a helical scan for head X-ray CT examination. X-ray CT unit has a bow tie filter that adjusts the X-ray intensity, and the X-ray beam has a fan angle that spreads in the transverse plane and spreads in the head-to-tail direction. For this reason, we have incorporated the photon number correspond the ratio of X-ray intensity distribution according to the fan angle of transverse plane and of head-to-tail direction in the simulation. In this study, the photon number was not making the same as the photon number in the actual head X-ray CT. The photon number was 1.8 billion, and we evaluated absorbed dose as a relative value. The distance between the X-ray focus and the axis of rotation was 60mm, the beam width in the head to-tail direction was 3.2mm, and the helical pitch was 0.95.

2.2 Voxel Phantom

We developed a voxel phantom using the actual CT images of a human phantom for CT (CTU-41) (Fig.1) made by KYOTO KAGAKU CO.LTD as the subject. CTU-41 is a human phantom that has 26 organs of the human as its structure, but it did not have lens structures. So we added the lens structures inside the eyeballs of the voxel phantom with reference to the literature [2]. In the phantom, two dosimeters were also incorporated on the eyelid surface. The number of voxels was $(x, y, z) = (145, 185, 42)$, and the voxel size was $(x, y, z) = (1.25\text{mm}, 1.25\text{mm}, 5\text{mm})$. Compositions of the lenses and eyeballs were set to ICRU-44 lens and water, respectively. To obtain sufficient deposition energy, the dosimeter material was set to soft-tissue, not to air or some kinds of dosimeter materials. After the deposit energy to the soft-tissue was obtained, it was converted to absorbed dose for air.

2.3 Formalism

After the simulation, using equation (1), deposit energy of lenses and dosimeters were converted to absorbed dose, respectively. The absorbed dose of dosimeters as soft-tissue was then converted to absorbed dose for air using equation (2). In addition, we obtained an absorbed dose distribution diagram on the axial plane of voxel phantom where the lenses and dosimeters exist (fig.2), and evaluated the relationship of absorbed dose between the lens and surrounding tissue, and its changes due to depth.

$$D = \frac{E \times 1.6 \times 10^{-13}}{V \times \rho} \quad (1)$$

D : Absorbed Dose (Gy)

V : Voxel Volume (cm^3)

E : Deposit Energy (eV)

ρ : Density (kg/cm^3)

$$D_{air} = D_{soft-tissue} \times \frac{(\mu/\rho)_{air}}{(\mu/\rho)_{soft-tissue}} \quad (2)$$

$(\mu/\rho)_{air}$: Mass Energy-Absorption Coefficient of AIR (cm^2/kg)

$(\mu/\rho)_{soft-tissue}$: Mass Energy-Absorption Coefficient of Soft-Tissue (cm^2/kg)

3. Results

Table 1 and 2 show the calculation results. In the Table 2, the ratios of the absorbed dose of the lens to the dosimeter were 0.77 on the right-eye side and 0.82 on the left-eye side. The ratio of the absorbed dose of the lens to the dosimeter at the eyelid position was approximately 0.8.

Fig.3 shows the absorbed dose distribution in the axial plane where the lenses and dosimeters exist. In the

homogeneous tissue region, the absorbed dose decreased with depth. In addition, the absorbed dose was low in the order of bone, soft-tissue (brain), water, lens and air. The absorbed dose of eyeball was lower than that of the surrounding soft-tissue and dosimeters.

Fig.4 shows the right eye part was displayed in a color code map correspond to the absorbed dose. The absorbed dose of the lenses was lower than that of the eyeball's area at the same depth.

4. Discussion

The result of this study shows that the absorbed dose of the lens was lower than that of the dosimeter on the eyelid surface. In general, in X-ray irradiation from one direction (front), it is known that the ratio of absorbed dose between the lens located 3mm deep from the eyelid surface and the dosimeter put on the eyelid surface is approximately 0.8 times, considering the factor of depth. Also, it is known that when the absorbed dose at the position on the surface of the human body is measured in free air, the absorbed dose that is added to the absorbed dose by the backscattered radiation is considered to the human surface dose. And, in the diagnostic energy region, the coefficient that takes into account the back scatter radiation component is regarded as 1.1~1.4. In this study, under the head X-ray Ct condition, which is the rotary irradiation, the ratio of the absorbed dose between the lens and the dosimeter on the eyelid was approximately 0.8. Because the phantom has a structure and organization that are very close to the human body, it is estimated that an effect in the actual human body will be equivalent to this result. So it is considered that when the dosimeter is put on the eyelid surface, the absorbed dose of the lens is calculated by multiplying the measurement value by 0.8. The CT-AEC (Auto Exposure Control) and the material and density of the bed differ depending on the X-ray CT unit, so we should consider the effects of these factors in the future.

The results of absorbed dose distribution showed that the absorbed dose decreased with depth from the body surface. The X-ray energy in the diagnostic area is lower than that in the treatment area and does not cause buildup of the absorbed dose. So the absorbed dose at the surface of the subject was high and decreases with depth from the surface. Moreover, the cause of decreasing in absorbed dose in the order of bone, soft-tissue (brain), water, lens, and air was the difference in mass energy-absorption coefficient. In particular, it is considered that the absorbed dose of brain was relatively low because the brain was covered with a highly absorbing skull and was deeply placed in the head.

5. Conclusion

In the Monte Carlo calculation, the absorbed dose ratio between the lens and the dosimeter placed on the eyelid was about 0.8 in head CT. Even in actual measurements, it was considered that the dose of the lens is smaller than the dose on the eyelid surface.

References

- 1) Hideo H, Yoshihito N. THE EGS5 CODE SYSTEM , KEK Report number:2005 8
- 2) H FERNER, J STAUBESAND Atlas der Anatomie des Menschen 1.Band: Kopf, Half, Obere Extremitaten, Sobatta, IGAKU-SHOIN Ltd. (in japanese)
- 3) Japanese Society of radiological technology, Photon attenuation coefficient data book, ISSN 1340-7716
- 4) KYOTO KAGAKU CO.LTD
<https://www.kyotokagaku.com/jp/educational/products/detail03/ph-4.html>,
or https://www.kyotokagaku.com/jp/educational/products/detail03/pdf/ph-4_catalog.pdf

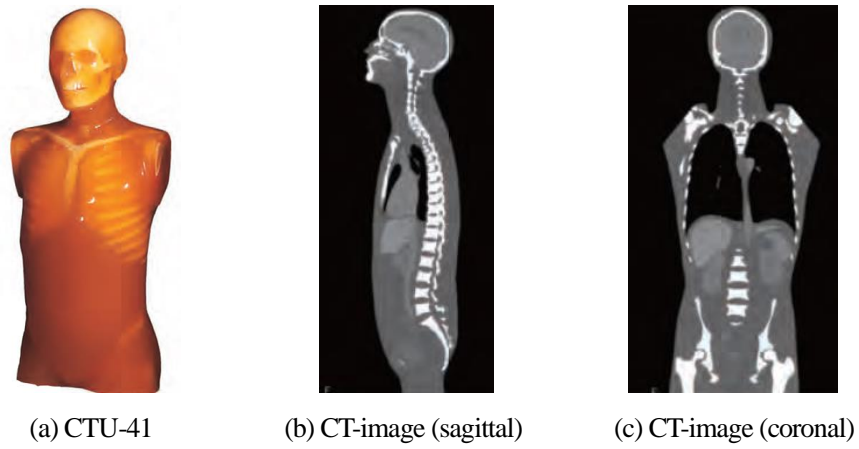


Fig.1 Human Phantom for CT (CTU-41, KYOTO KAGAKU CO.LTD [4])



Fig.2 An axial plane of voxel phantom

Table 1 Calculate result

	Relative absorbed dose (mGy)	
	right-eye	left-eye
lens	0.0008126	0.0008153
dosimeter (air)	0.001051	0.0009908

Table 2 The ratio of absorbed dose

	right-eye	left-eye
The dose ratio between the lens and the dosimeter (air)	0.7733	0.8229

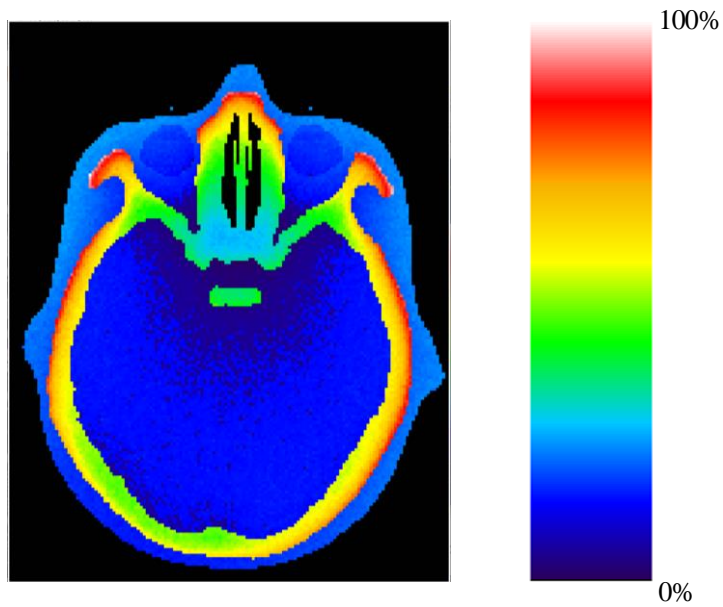


Fig.3 Dose distribution (Color code map)

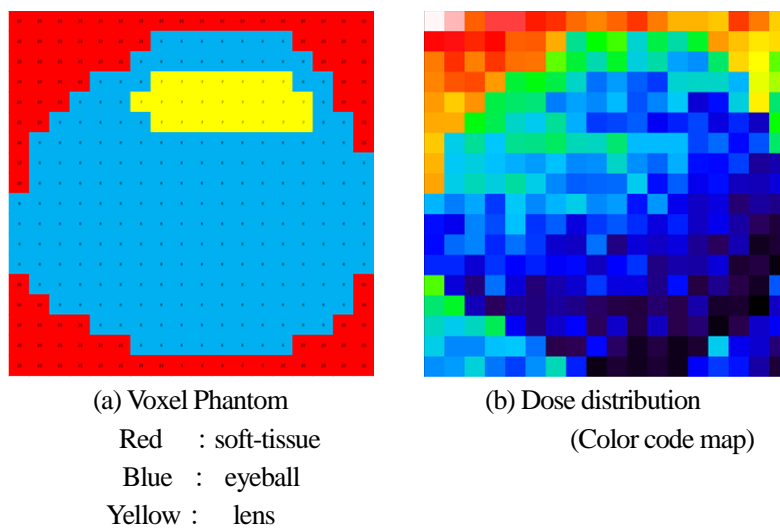


Fig.4 Right eyeball dose distribution

Use of ICRU90 density effect parameter in EGS5

Y. Namito¹, H. Hirayama¹ and M. Shimizu²

¹ KEK, Tsukuba Ibaraki 305-0801, Japan

² AIST, Tsukuba Ibaraki 305-8560, Japan

e-mail Yoshihito.namito@kek.jp

Abstract

Since the densities in the calculation of the electron stopping power and the densities in the calculation of the density effect should normally match, in order to prevent inadvertent dissociation between the two, an error will occur if they deviate by 1% or more with pgs5 input. A message is output and abnormally stopped. On the other hand, as a new method in ICRU90, we accept that there is a difference of 1% or more between the two. Therefore, we changed the input method of density effect data in pgs5 and the related parts of pgs5 to allow input by this new way. Specifically, if you intentionally use different values for both, specify the density in the density effect file with a negative value. And pgs5 ignores the difference from the density in pgs5 input when reading negative density from density effect input file.

1. Introduction

The density effect is a phenomenon in which the material is polarized due to incident electrons and the collision stopping power is reduced. For carbon, for example, the maximum reduction is as large as 14% of the total stopping power, and accurate treatment of the density effect is important. For this reason, egs5 [1] deals with the density effect in three ways. The first method is the general treatment of Sternheimer & Peierls, which is a little less accurate with a total stopping power error of <2%, but it can be handled only with Z and ρ and is simple [2]. The second method is to use the parameters of 278 substances by Sternheimer, Berger, and Seltzer [3]. The third method is to use the value of ICRU-37 [4]. In this case, since the density effect at 49 energy points is specified, it can be handled with the highest precision. However, it is complicated because it is necessary to prepare a density effect file for each substance.

Graphite is used as a material for the ionization chamber and is an important material in radiation measurement, and has a large density effect. Since the density and the average ionization energy influence the density effect, it is necessary to use accurate values of the density and the average ionization energy in order to obtain an appropriate value of the density effect. However, there is a problem that the density of graphite varies widely, and that a high density graphite is easily cracked

and has low workability. Therefore, how to handle the density and density effect of graphite is an important issue in radiation physics, and has been repeatedly taken up in the ICRU Report. In ICRU37, the problem of stopping power of non-homogeneous materials such as graphite was raised, and the stopping powers of 1.7 g cm^{-3} and 2.265 g cm^{-3} were posted, and the use of 1.7 g cm^{-3} was recommended. ICRU49 also posted carbon stopping powers of 1.7 g cm^{-3} and 2.0 g cm^{-3} [5].

2. NRC PIRS-0626 and ICRU90

NRC PIRS-0626 states that "calculating the density effect of graphite using 2.265 g cm^{-3} reproduces experimental values well" [6]. According to this claim, "The average stopping power is obtained by measuring the density, but the collision phenomenon with atoms occurs only in the crystal part. The density effect is inconsistent unless calculated by the density of the crystal part." The handling of the density effect of ICRU90 follows this idea [7]. In order to perform the calculation as claimed, different densities are used as the density of the whole substance and the density when calculating the density effect. The ICRU Report 90 states that "bulk density rarely exceeds 1.8 g cm^{-3} and grain density is 2.265 g cm^{-3} ". It is necessary to confirm the actual bulk density before the calculation. A corrected version of NIRC PIRS-0626 was published, and the densities of ordinary graphite and pyrolytic graphite used for measurement were shown to be 1.7 g cm^{-3} and 2.2 g cm^{-3} , respectively [8].

3. How to use ICRU90 density effect data in egs5

Since the densities in the calculation of the electron stopping power and the densities in the calculation of the density effect should normally match, when pgs5 input deviates by 1% or more, an error message is output and abnormal termination is performed. This is to prevent inadvertent discrepancy between the two densities. However, as stated above, the idea of ICRU90 allows for a difference of 1% or more between the two. Therefore, we changed the input method of density effect data in pgs5 and the corresponding pgs5 so as to allow the input based on this way of thinking while maintaining the check function for the deviation of both densities due to carelessness. Specifically, if you intentionally use different values for both, specify the density in the density effect file with a negative value, and if pgs5 reads a negative density, set it to a positive value. After conversion, we decided to accept the difference from the density in the pgs5 input.

Example of first three lines of PEGS5 input (including density specification for stopping power calculation):

ELEM

```
&INP RHO=1.85, IUNRST=1, EPSTFL=1 &END
graphite_icru90
```

IUNRST=1 is used to output unrestricted collision stopping power shown below and it should be erased in usual MC calculation.

Example of first two lines of EPSTAR file (including density specification for density effect data):

```
graphite_icru90
49 81.0 -2.265 1 6 1.000
```

The epstar file is a file used in EGS5 to use ICRU37 density effect data. Even when using ICRU90 density effect data, it is necessary to create a density effect file for each substance, combine it, and create a file called epstar. There is no problem if ICRU90-based and ICRU37-based density effect data are mixed in one epstar file. The following changes have been made to pegas5:

```
4807a4808,4812
> !      18Jun2020 Kludge by Y.Namito to use different rho in epstar&pegas5 input
>      if (EPSTRH .lt. 0.0) then
>          TLRNCE=1.0
>          EPSTRH=ABS(EPSTRH)
>      end if
```

If the value of EPSTRH (the variable that reads the density in the density effect data) is negative, change EPSTRH to a positive value to allow up to 100% difference from the density in the pegas5 input for the stopping power calculation. Therefore, the confirmation of the difference between the two is substantially nullified. The pegas5 and EPSTAR files with this change are released as one of the add-on of egs5 HP, so the user can use this file as it is.

When S_{el}/ρ was calculated with the above-mentioned PEGS5 input and EPSTAR input, and compared with the values in Table A.2. of ICRU90, the values well matched as shown in the table below were obtained.

T MeV	S_{el}/ρ MeV cm ² g ⁻¹	
	Table A.2. ICRU90	PEGS5 output
0.001	1.048E+02	1.047E+02
0.01	1.999E+01	1.999E+01
0.1	3.654E+00	3.654E+00
1.0	1.606E+00	1.606E+00
10	1.729E+00	1.729E+00

100	1.928E+00	1.928E+00
1000	2.106E+00	2.105E+00

References

- 1) H. Hirayama, Y. Namito, A. F. Bielajew, S. J. Wilderman, and W. R. Nelson: "The EGS5 Code System", SLAC-R-730 and KEK Report 2005-8 (2005).
- 2) R. M. Sternheimer and R. F. Peierls: "General expression for the density effect for the ionization loss of charged particles". Phys. Rev. B **3**, 3681, (1971) through KEK Report 2005-8.
- 3) R. M. Sternheimer, M. J. Berger, and M. Seltzer: "Density effect for the ionization loss of charged particles in various substances", At. Data and Nucl. Data Tables, **30**, 261 (1984).
- 4) International Commission on Radiation Units and Measurements: "Stopping Powers for Electrons and Positrons", ICRU Report 37 (1984).
- 5) International Commission on Radiation Units and Measurements: "Stopping Power and Ranges for Protons and Alpha Particles", ICRU49 (1993); through ICRU Report 90.
- 6) M. S. MacPherson: "Accurate measurements of the collision stopping powers for 5 to 30 MeV electrons", Ph.D. dissertation, Carlton Univ., Ottawa, and NRC Report NRC PIRS-0626 (1998). <https://doi.org/10.4224/40000364>
<https://nrc-publications.canada.ca/eng/view/object/?id=bcf26036-6ec7-4520-bc5c-201387404393> Last access on 29Jun2020.
- 7) International Commission on Radiation Units and Measurements: "Key Data for Ionizing-Radiation Dosimetry: Measurement Standards and Applications", ICRU Report 90 (2014).
- 8) F. Tessier, and C. K. Ross: "Correction to report PIRS-0626 on electron stopping powers", NRC (2019).
https://www.researchgate.net/profile/Carl_Ross5/publication/330912208_Corrections_to_report_PIRS-0626_on_electron_stopping_powers/links/5c5b334545851582c3d3cc17/Corrections-to-report-PIRS-0626-on-electron-stopping-powers.pdf Last access on 3Jul2020.

Appendix A. Effect of ρ and I to stopping power

Effect of density ρ and mean ionization potential I to stopping power is summarized. The stopping power is divided into 1) density effect part and 2) the part other than density effect. The density effect part depends on both ρ and I , whereas the part other than the density effect does not depend on ρ but on I .

The ρ in the second line of the EPSTAR file records the values used for the calculation of density

effect parameter which is shown on the third and subsequent lines. Rewriting this ρ does not affect the calculation result (*¹) because this ρ was already used for the calculation. On the other hand, I in the second line has two meanings. First, this value of I was used for calculating the density effect parameter and it is written as a record (*²). Second, I in the second line is also used for calculation of the part of the stopping power other than the density effect (*³). Therefore, changing this I will affect the calculation results.

Stopping power (MeV cm ² g ⁻¹)	Density ρ	Mean ionization potential I
Density effect part	○* ¹	○* ²
Other than the density effect part	×	○* ³

In Fig4.2 of ICRU90, the calculation of the first condition ($\rho=2.265 \text{ g cm}^{-3} : I=78\text{eV}$) and the second condition ($\rho=1.7 \text{ g cm}^{-3} : I=78\text{eV}$) of ICRU37 is compared with the experiment, and the former is closer to the experiment. Then 2.265 g cm^{-3} is recommended. However, ICRU90 recommends $I=81 \text{ eV}$, and eventually ICRU90 recommends the third condition ($\rho=2.265 \text{ g cm}^{-3} : I=81 \text{ eV}$). As mentioned above, both ρ and I affect the stopping power, so the difference in the stopping power between the first condition and the third condition must be considered. The difference is 0.1% or less at 20 MeV comparing with the experiment and 1.4% at 1 keV not comparing with the experiment. There is no difference in terms of agreement with experiment.

Note that using the density in the pegas5 input, (mass) stopping power in unit of MeV cm² g⁻¹ is converted into stopping power in unit of MeV cm⁻¹ and output as pegas5 data.

Appendix B. Method that we did not adopt after all

In order to solve this problem, we initially thought of using the function to specify the density for each area in the user code. In this case, in the PEGS5 input, write the same density as the density effect file, and specify the bulk density that you want to actually use in the calculation as the density for each area.

Before HATCH CALL in user code, we write

```
RHOR()=1.85
```

It is a method of inputting the actual density at the time of calculation and scaling the stopping power. However, this method was not adopted because the Goudsmit-Saunderson multiple scattering distribution cannot be used in this case.